

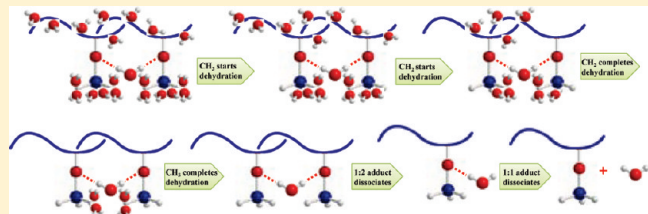
Integrated Microdynamics Mechanism of the Thermal-Induced Phase Separation Behavior of Poly(vinyl methyl ether) Aqueous Solution

Bingjie Sun, Hengjie Lai, and Peiyi Wu*

The Key Laboratory of Molecular Engineering of Polymers, Ministry of Education, Department of Macromolecular Science, and Laboratory of Advanced Materials, Fudan University, Shanghai 200433, People's Republic of China

ABSTRACT: The thermal behavior of a poly(vinyl methyl ether) (PVME) aqueous solution (30 wt %) during a heating-and-cooling cycle is studied using FTIR spectroscopy in combination with 2D correlation analysis. The FTIR spectral data of O–H, CH₃–O, and C–H stretching vibration regions provide detailed changes of hydrophilic and hydrophobic groups of PVME. Hydrogen bonds between hydrophilic groups and water and hydration interactions between hydrophobic groups and water are confirmed to be completely reversible in the heating-and-cooling cycle. Two-dimensional correlation method helps us to understand the microdynamics mechanism of phase separation behavior of PVME 30 wt % aqueous solution. During the heating process, the initially hydrated CH₃ groups start to dehydrate as the first action of phase separation, and the initially hydrated CH₂ groups follow to start their dehydration; interestingly, water molecules leave CH₂ groups very fast, and the whole dehydration process of CH₂ groups finishes even earlier than that of CH₃. After hydrophobic groups finish their dehydrations, hydrogen bonds between hydrophilic group and water start to dissociate. 1:2 adducts formed between PVME and water dissociate first and transfer to the 1:1 adducts, whereas with further heating, 1:1 adducts eventually dissociate and release free water and free CH₃–O. PCMW method is used as supplement to determine changing conditions of various chemical structures. During the phase separation, O–H hydrogen bond in 1:2 adduct is found to dissociate between 35.5 and 39 °C in a

style, whereas the 1:1 adduct (also considered as free water) increases between 35.5 and 39 °C in a style. Moreover, dehydration conditions of hydrophobic groups are also found. Both of the dehydrated states CH₃ and CH₂ increase like



INTRODUCTION

Poly(vinyl methyl ether) (PVME) (chemical structure shown in Figure 1a) is a water-soluble polymer that is sensitive to environmental temperature.¹ Hydrophobic and hydrophilic groups in PVME play different roles at various temperatures, which makes this polymer undergo a phase separation behavior at a lower critical solution temperature (LCST) around 37 °C in the aqueous solution. Below the LCST, hydrophobic CH₃ and CH₂ groups interact with water clusters by hydration effect,² whereas hydrophilic CH₃–O groups interact with water by hydrogen bonds, potentially forming two kinds of adducts, 1:1 and 1:2 adducts, as shown in Figure 1b;³ hydrogen bonds between ether oxygen and water in these adducts are much stronger than the whereas hydrogen bonds between hydrophilic group and water break down. Evolution of hydrophobic and hydrophilic groups during the heating process is the driving force of phase separation in the PVME aqueous solution.^{3a}

A great deal of research has been done to investigate the phase separation process of PVME; techniques like nuclear magnetic resonance,⁴ small angle neutron scattering,⁵ dielectric

investigations,⁶ DSC,^{1d,7} simulations,⁸ and Raman spectroscopy⁹ were used. Among these, IR spectroscopy is a more effective method in investigating changes of conformations, interactions, and microenvironments of individual chemical groups during phase separation.^{3a,9a,10} For example, Maeda observes that heating of the PVME solution above the LCST leads to red shifts of C–H stretching bands and blue shift of the C–O stretching band, which indicates that hydrophobic groups dehydrate and hydrogen bonds between hydrophilic group and water break down during the heating process.^{10c} Our group has investigated the thermal sensitivities of PVME by near-infrared (NIR) and 2D correlation spectroscopy, finding that the dehydration of hydrophobic groups starts earlier than breakage of hydrogen bonds between hydrophilic group and water.^{3a} However, because of the requirement of high sample thickness in NIR experiments, opacification of PVME aqueous solution after phase separation

Received: July 16, 2010

Revised: November 15, 2010

Published: January 24, 2011

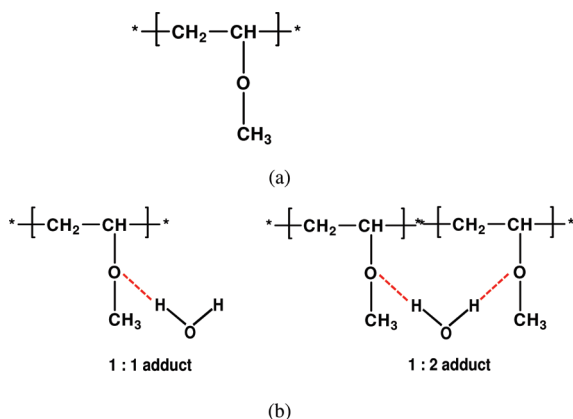


Figure 1. (a) Chemical structure of PVME. (b) Structures of potential adducts formed between PVME units and water molecules in PVME aqueous solution.

makes it almost impossible to obtain NIR spectra above LCST. Therefore, more reliable spectra information still needs to be acquired to understand the whole phase separation process.

Generalized 2D correlation spectroscopy was originally proposed by Noda in 1993;¹¹ this method enables the investigation of spectral intensity fluctuations under an external perturbation like temperature,¹² time,¹³ pH,¹⁴ concentration,¹⁵ and so on. By spreading peaks over the second dimension, 2D spectra can also greatly improve the spectral resolution; for example, they can separate overlapped peaks in the 1D spectra and discern the exact vibration positions of peaks, which is very important for understanding the accurate microstructures of chemicals. As a supplement of 2DIR, newly developed Perturbation correlation moving window (PCMW) technique is proposed by Morita.¹⁶ This method introduces the perturbation variable to the correlation equation and enables us to determine exact transition points of complicated spectral variations.

Despite wide applications of FTIR spectroscopy for investigating the phase separation behavior of PVME aqueous solution, the integrated phase separation microdynamics mechanism on the molecular level still remains a blank; researchers have shown that the dehydration of hydrophobic groups and breakage of the hydrophilic group evolved hydrogen bonds by lots of evidence, but changing orders between these two events are seldom directly told. Moreover, both hydrophobic groups of CH_3 and CH_2 dehydrate during phase separation,^{10c} whereas which happens or ends earlier has never been told. Additionally, previous NIR work of our group has given only the spectroscopic information during 25–33 °C;^{3a} further information related to the main phase separation process around LCST is on demand.

In the present work, we study the thermal-induced behavior of PVME 30 wt % aqueous solution by mid-infrared spectroscopy, which enables us to obtain spectra in the heating-and-cooling cycle between 33 and 41 °C. O–H, C–H, and CH_3 –O stretching vibration regions in the FTIR spectra are investigated, and changes of hydrophobic and hydrophilic groups during the heating–cooling cycle are obtained. More important, the microdynamics mechanism of various structures in PVME aqueous solution during the whole phase separation process is effectively analyzed by 2DIR correlation spectroscopy. This provides us with deeper understanding of structure–property relationships of the temperature-sensitive polymers. We also find the

beginning, transition, and ending temperatures of various structure changes with the help of the PCMW method.

EXPERIMENTAL SECTION

Materials and Sample Preparation. PVME in a 30 wt % aqueous solution was obtained from Tokyo Kasei Kogyo. The sample was used without any further treatment. After being lyophilized for 48 h, the roughly estimated molecular weight of the polymer was determined by gel permeation chromatography (GPC) (HP1100) using three Waters Styragel columns and a Waters 410 refractive-index detector and THF as eluent with a flow rate of $1 \text{ mL}\cdot\text{min}^{-1}$ at 35 °C. Monodisperse polystyrene was used as the calibration standard. The PVME sample had an $M_w = 6500$ and an $M_w/M_n = 2.58$.

Fourier Transform Infrared Spectroscopy. The FTIR spectra were recorded with a 4 cm^{-1} spectral resolution on a Nicolet Nexus 470 spectrometer equipped with a DTGS detector by signal-averaging 128 scans. Microscope CaF₂ windows, which have no absorption bands above 1100 cm^{-1} in the MIR region, were used to prepare a transmission cell. Variable-temperature spectra were collected between 33 and 41 °C with an increment of 1 °C (accuracy: 0.1 °C). The manual method was used to change the temperature; for complete equilibrium, each temperature point was maintained for 30 min to collect the IR spectrum, and then the temperature was increased or decreased for 1 °C manually. The baseline correct processing of O–H, C–H, and CH_3 –O stretching vibration bands was performed by the software of OMNIC 8.0.

Two-Dimensional Correlation Analysis. Spectra recorded at an interval of 1 °C were selected in certain wavenumber ranges, and the generalized 2D correlation analysis was applied by 2D Shige software (Shigeaki Morita, Kwansei-Gakuin University, Japan) and drawn by Origin 8.0 software. To avoid the risk of overinterpretation and the loss of useful information, an appropriate number of level (the parameter in Origin 8.0 software) has been set up in our experiments. In 2D correlation maps, red system-colored regions (yellow-red) are defined as positive correlation intensities, whereas blue system-colored regions (cyan-blue) are regarded as negative correlation intensities. A window size of $2m + 1 = 5$ is chosen to generate PCMW spectra.

RESULTS AND DISCUSSION

One-Dimensional Fourier Transform Infrared Spectroscopy Study. Temperature-dependent FTIR spectra of PVME 30 wt % aqueous solution (33–41 °C heating-and-cooling cycle) are shown in Figure 2. Stretching vibration regions of O–H, C–H, and CH_3 –O are mainly investigated in the present study. Peaks in the spectra and their corresponding assignments are listed in Table 1.^{3,9b,10c} Because of overlapping, exact wavenumbers of certain peaks cannot be clearly observed in 1D spectra, and these positions are confirmed by 2DIR spectra analyzed below.

O–H Stretching Vibration Region. The 3800–3012 cm^{-1} region is related to the stretching vibration of O–H groups. Maeda^{10b} reported that free water (i.e., water not disturbed by PVME) did not exist above 38 wt % PVME aqueous solution. Because the concentration of the sample used in this study is 30%, the water molecules in our study could be roughly categorized into two subgroups: those that interacted with PVME (disturbed water) and those that did not interact with

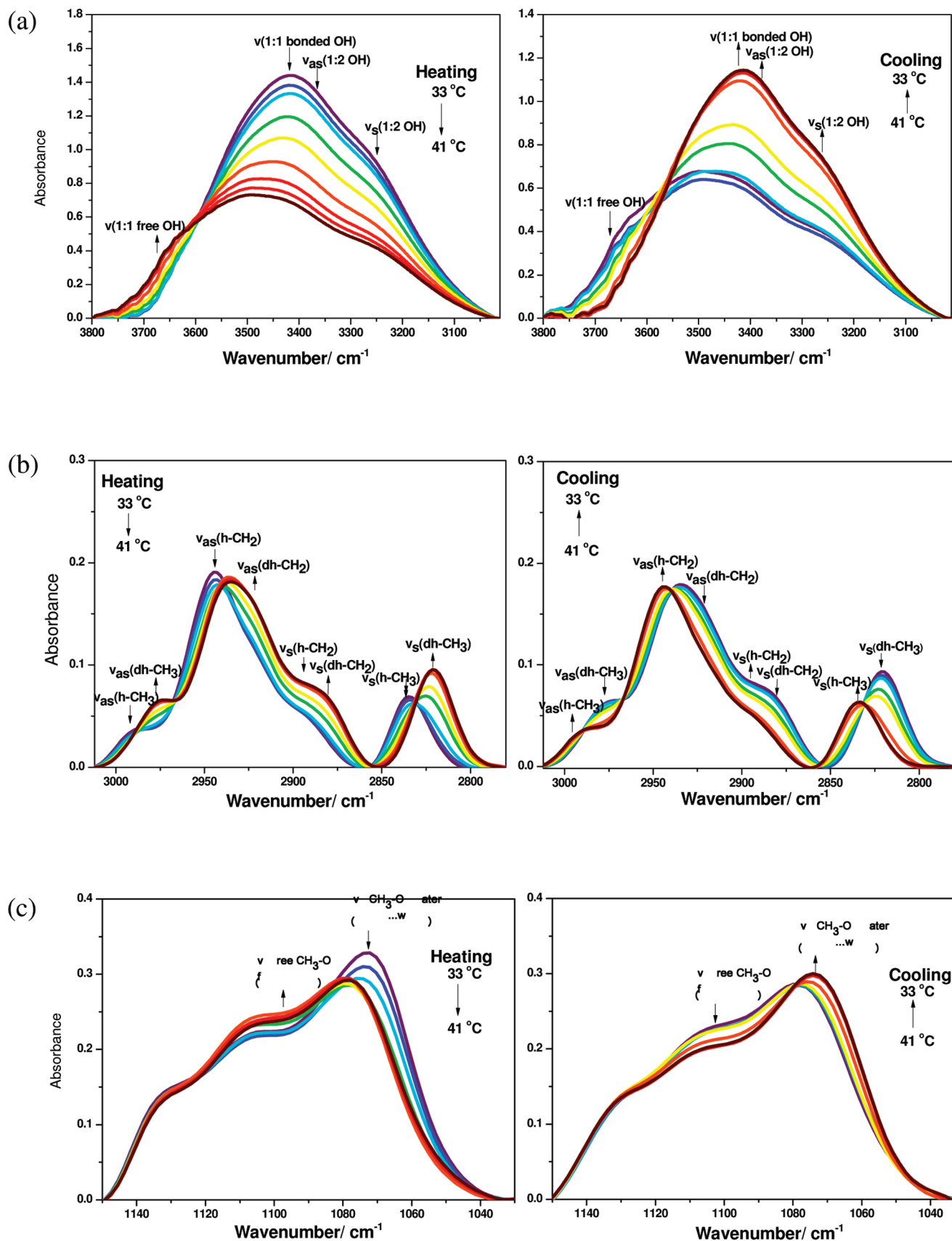


Figure 2. FTIR spectra of PVME 30 wt % aqueous solution during heating-and-cooling cycle. (a) O–H stretching vibration region. (b) C–H stretching vibration region. (c) $\text{CH}_3\text{-O}$ stretching vibration region. The temperature was varied between 33 and 41 °C with an interval of 1 °C.

Table 1. Assignments of PVME in Aqueous Solution in the C—H and C—O Vibration Regions of MIR Spectra in Whole Temperature Range^{3,9b,10c,a}

wavenumber (cm^{-1})	assignment
3660	free OH in 1:1 adduct (also considered as in free water)
3442	bonded OH in 1:1 adduct
3392	$\nu_{\text{as}}(\text{OH})$ in 1:2 adduct
3278	$\nu_s(\text{OH})$ in 1:2 adduct
2996	$\nu_{\text{as}}(\text{h-CH}_3)$
2973	$\nu_{\text{as}}(\text{dh-CH}_3)$
2950	$\nu_{\text{as}}(\text{h-CH}_2)$
2924	$\nu_{\text{as}}(\text{dh-CH}_2)$
2890	$\nu_s(\text{h-CH}_2)$
2879	$\nu_s(\text{dh-CH}_2)$
2839	$\nu_s(\text{h-CH}_3)$
2817	$\nu_s(\text{dh-CH}_3)$
1135	$\nu(\text{C-O}) + \nu(\text{C-C})$
1105	$\nu(\text{C-O}) + r(\text{C-H})$
1095	$\nu(\text{free CH}_3-\text{O})$
1066	$\nu(\text{CH}_3-\text{O}\cdots\text{water})$

^a h- is for hydrated, dh- is for dehydrated. Because of overlapping, positions of certain bands cannot be accurately gained in 1D spectra, and their exact positions are ascertained by 2DIR analysis.

PVME (bulk or free water). However, usually, the change of the bulk water (not disturbed with PVME) during the temperature range (33–41 °C) is relatively small in contrast with the very large change of disturbed water (those that interacted with PVME) during the phase separation process.

The OH-stretching area exists as a whole broad band in Figure 2a, showing the existence of many overlapped bands. On the basis of a previous study of our group,^{3a} we have known that water molecules can interact with hydrophilic CH_3-O groups in PVME and potentially form two kinds of adducts (1:1 and 1:2),³ shown in Figure 1b. Hence, there might be four different OH vibration modes for the disturbed water: free O—H in 1:1 adduct (similar as O—H vibration in bulk water, usually appears around 3660 cm^{-1}), bonded O—H in 1:1 adduct (3442 cm^{-1}), and $\nu_{\text{as}}(\text{OH})$ and $\nu_s(\text{OH})$ in 1:2 adduct (around 3392 and 3278 cm^{-1}).³ Because of the overlapping of these four peaks, it is very difficult to study them accurately based on 1D FTIR spectra. We will discuss more about various OH vibrations in the following 2DIR part. To remove the thermal effect of water, we compare the temperature-dependent variation of overall $\nu(\text{OH})$ band in pure water and PVME/water and find that the changes (i.e., change of shape, intensity, and peak position) of $\nu(\text{OH})$ band in pure water in heating process are limited. In contrast, we could clearly observe that the overall $\nu(\text{OH})$ band in PVME water solution shows a typical sigmoid curve during heating and cooling. We quantitatively analyze the temperature dependence of these shifts in Figure 3a. Previous study shows that blue shift of $\nu(\text{NH})$ or $\nu(\text{OH})$ bands indicates the weakening of hydrogen bonds formed by NH or OH,^{12c} so red shift of those bands testified the strengthening of those hydrogen bonds. In PVME aqueous solution, water interacts with CH_3-O of PVME and forms relatively strong hydrogen bonds; therefore, according to the shifts of $\nu(\text{OH})$ band in the heating–cooling cycle, we can infer that during heating hydrogen bonds between water and

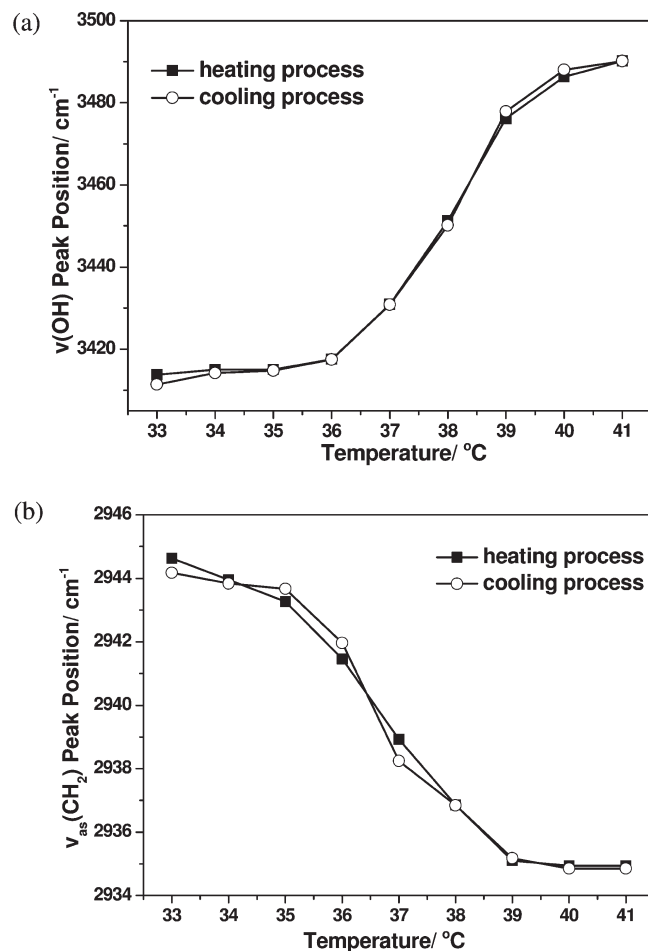


Figure 3. Peak positions of (a) $\nu(\text{OH})$ and (b) $\nu_{\text{as}}(\text{CH}_2)$ in the FTIR spectra of PVME 30 wt % aqueous solution as a function of temperature. The temperature of the heating-and-cooling cycle was varied between 33 and 41 °C with an interval of 1 °C. Filled symbols represent the heating process and open symbols represent the cooling process.

CH_3-O weaken or break down, whereas during cooling, these hydrogen bonds are strengthened or formed again. Changes of these hydrogen bonds are one of the main driving forces of the phase separation behavior of PVME aqueous solution.

Meanwhile, by studying exact wavenumbers of $\nu(\text{OH})$ at different temperatures in Figure 3a, we find that peak positions at the same temperature in heating and cooling have good consistency; there is no hysteresis between these two thermal processes. This means that the formation/strengthening rate and the dissociation/weakening rate of $\text{CH}_3-\text{O}\cdots\text{water}$ hydrogen bonds are almost the same. This phenomenon is different from what we have learned in another temperature-sensitive polymer—PNIPAM.^{12d} There are two hydrophilic group in PNIPAM, C=O and N—D (N—H after deuterated), and both of them interact with water in aqueous solution below LCST. During heating of PNIPAM 20 wt % D₂O aqueous solution, hydrogen bonds between hydrophilic group and water (C=O···D₂O and N—D···D₂O) break, and new inter/intra-chain hydrogen bonds C=O···D—N are formed, whereas during cooling, C=O···D—N hydrogen bonds dissociate and hydrogen bonds of C=O···D₂O and N—D···D₂O are formed again. However, according to the quantitative study, we observe that the dissociation of C=O···D—N is slower than its

formation. The hysteresis is due to the great strength of $\text{C}=\text{O}\cdots\text{N}-\text{H}$ hydrogen bonds; such hydrogen bonds cannot easily break down in the cooling process so that they postpone PNIPAM aqueous solution reversing to the initial state, whereas in PVME 30 wt % aqueous solution, $\text{CH}_3-\text{O}\cdots\text{water}$ hydrogen bonds form/strengthen and dissociate/weaken in the same rate. A possible reason for this difference between PNIPAM and PVME is that there is only one hydrophilic group in PVME, after the phase separation hydrogen bonds of $\text{CH}_3-\text{O}\cdots\text{water}$ break, and no new inter/intrachain hydrogen bonds will be formed. Therefore, there is not any effect that will hinder the reverse of the whole system in the cooling process. On the basis of this view, we can infer that the phase separation mechanisms between PNIPAM and PVME are essentially different. PVME displays a type III LCST demixing behavior in water at certain temperatures according to one type of polymer/solvent phase diagrams. This behavior is characterized by the presence of two off-zero limiting critical concentrations.¹⁷

C–H Stretching Vibration Region. The region of $3012\text{--}2780\text{ cm}^{-1}$ refers to vibrations of C–H groups; the assignment of CH_x stretching vibrations in PVME is rather complicated and uncertain in the existing literature. In their Raman spectroscopic study, Pastorcak et al.^{9b} gave a very detailed assignment of CH_x stretching vibrations in PVME gel. The tentative assignments of the major CH_x stretching bands are listed in Table 1, similar to the results of Pastorcak et al.^{9b} However, we tend to assign the 2924 cm^{-1} band to be the dehydrated state of CH_2 group because of its similar dynamic behavior to 2973 cm^{-1} (dehydrated state of CH_3) and opposite dynamic behavior of 2950 cm^{-1} (hydrated state of CH_2). The latter two assignments are clearly mentioned in Maeda's previous paper.^{10c} We can observe in Figure 2b that during the heating process CH_3 and CH_2 bands shift to lower wavenumber, whereas during the cooling process they undergo blue shift and reverse to the original high wavenumber. It is well known that CH_3 and CH_2 of PVME interact with water molecules at room temperature, and this hydration effect will be weakened upon heating. Red shifts of these peaks during heating reveal dehydration of CH_3 and CH_2 ,^{10c} and blue shifts during cooling manifest new hydration interactions that are formed between these C–H groups and water. Among all C–H vibration bands, the $\nu_{\text{as}}(\text{CH}_2)$ band has the most remarkable shift; we take it, for example, to analyze quantitatively the temperature dependence of C–H vibration peaks in Figure 3b.

At the beginning of heating, $\nu_{\text{as}}(\text{CH}_2)$ locates at 2944 cm^{-1} , whereas it performs a significant red shift around LCST, representing great dehydration effect of CH_2 . In the cooling process, $\nu_{\text{as}}(\text{CH}_2)$ performs a blue shift, which is more prominent around LCST; moreover, the $\nu_{\text{as}}(\text{CH}_2)$ peak finally reverses to its initial 2944 cm^{-1} position after complete cooling. This closed peak-shift cycle without any hysteresis helps us to conclude that the dehydration and hydration of C–H groups are almost completely reversible in the heating–cooling cycle. This confirms what we have learned in the O–H vibration region above. Because no inter/intrachain hydrogen bonds are formed after phase separation of PVME aqueous solution, the reverse of the whole system in the cooling process can be achieved easily. On the basis of shifts of O–H and C–H vibration peaks in Figure 3, we can conclude that changes of hydrogen bonds between hydrophilic group and water and changes of hydration effects between hydrophobic groups and water are completely reversible in PVME 30 wt % aqueous solution during the heating–cooling cycle.

CH_3-O Stretching Vibration Region. The $1150\text{--}1030\text{ cm}^{-1}$ region is related to the stretching vibration of CH_3-O groups, changes of this region are shown in Figure 2c. There are also many overlapped peaks, among which 1066 and 1095 cm^{-1} peaks change more significantly during the heating–cooling cycle. The 1066 cm^{-1} peak is assigned to $\nu(\text{CH}_3-\text{O})$ in $\text{CH}_3-\text{O}\cdots\text{water}$ hydrogen bonds, whereas the 1066 cm^{-1} peak is assigned to the vibration of free CH_3-O . The other two combination peaks $\nu(\text{C}-\text{O}) + \nu(\text{C}-\text{C})$ and $\nu(\text{C}-\text{O}) + r(\text{C}-\text{H})$ also exist in this region but have little change upon temperature variations.^{10c}

In Figure 2c, on one hand, the intensity of the 1066 cm^{-1} peak decreases, but that of the 1095 cm^{-1} peak increases during heating, inferring that the $\text{CH}_3-\text{O}\cdots\text{water}$ interaction dissociates and releases free CH_3-O in the phase separation process; on the other hand, the intensities of 1066 and 1095 cm^{-1} peaks change oppositely during cooling, which manifests the $\text{CH}_3-\text{O}\cdots\text{water}$ interaction can be formed again. Because CaF_2 is used as the window material in FTIR experiments, it has some absorbance below 1100 cm^{-1} . Therefore, for better accuracy, only qualitative analysis is done to spectra data of CH_3-O stretching vibration region.

2DIR Correlation Method. The 2DIR correlation spectra are characterized by two independent wavenumber axes (ν_1, ν_2) and a correlation intensity axis. In a pair of 2D spectra, synchronous and asynchronous maps are generally obtained. The correlation intensity in 2D synchronous and asynchronous maps reflects the relative degree of in-phase or out-of-phase response, respectively.

2D synchronous spectra are symmetric with respect to the diagonal line in the correlation map. Peaks appearing along the diagonal are called autopaks $\Phi(\nu_1, \nu_1)$, which are always positive. Autopaks represent the degree of autocorrelation of perturbation-induced molecular vibrations so that if there is an autopak at ν_1 , it means the peak at the same wavenumber of ν_1 in 1D spectra changes greatly under the environmental perturbation. Off-diagonal peaks are named cross peaks $\Phi(\nu_1, \nu_2)$, which represent the simultaneous or coincidental changes of spectra intensity variations measured at ν_1 and ν_2 . Cross peaks may be positive or negative, positive cross peaks $\Phi(\nu_1, \nu_2)$ demonstrates intensity variations of peak ν_1 and ν_2 take place in the same direction (both increase or decrease) under the perturbation; while negative cross peaks help to infer that intensities of peak ν_1 and ν_2 change in opposite directions (one increases, whereas the other one decreases).

The 2D asynchronous spectra are asymmetric with respect to the diagonal line. Unlike synchronous spectra, only off-diagonal cross peaks would appear in asynchronous spectra, and these cross peaks can also be either positive or negative. The intensity of cross peaks $\Psi(\nu_1, \nu_2)$ in the asynchronous map represents sequential or successive changes of spectral intensities observed at ν_1 and ν_2 . With the cross peaks that appear in both synchronous and asynchronous maps, we can figure out the specific changing orders of different peaks under the external perturbation. According to Noda's rule,¹¹ if cross peaks (ν_1, ν_2) in the synchronous and asynchronous maps have the same symbol, both positive or both negative, then we can conclude that peak ν_1 varies prior to peak ν_2 with the perturbation; whereas if cross peaks (ν_1, ν_2) in the synchronous and asynchronous maps have different symbols, one positive and the other one negative, then we can conclude that peak ν_2 varies prior to peak ν_1 . In the 2DIR throughout this Article, red system-colored (yellow-red) areas represent positive cross peaks, and blue system-colored (cyan-blue) areas represent negative cross peaks.

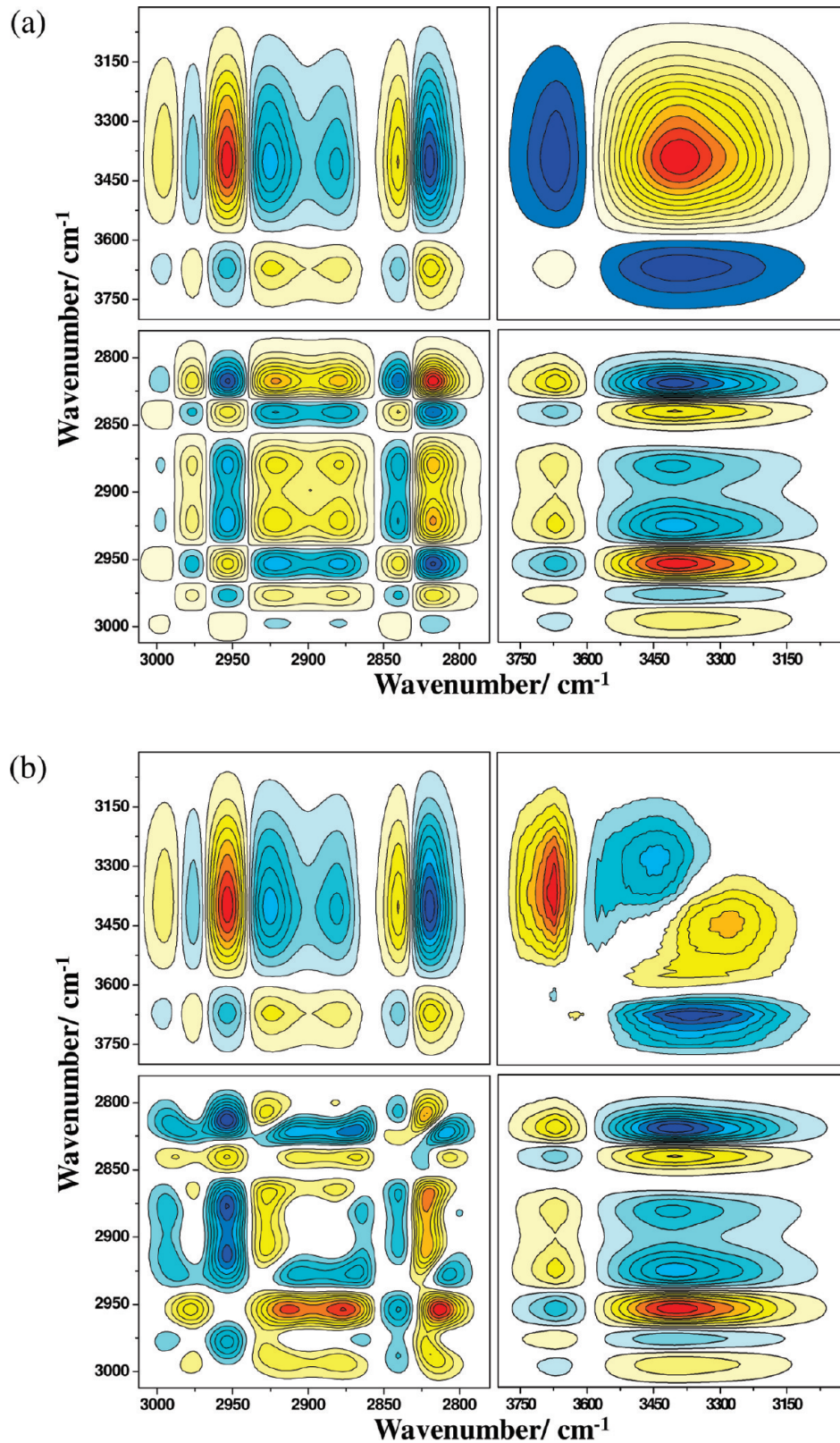


Figure 4. (a) Synchronous and (b) asynchronous 2DIR maps in the $\nu(\text{OH})$ region, the $\nu(\text{CH})$ region, and their cross regions obtained during the phase separation process of PVME 30 wt % aqueous solution.

PCMW Method. PCMW 2D analysis method correlates the external perturbation directly with infrared peaks so that it enables us to determine exact critical conditions,¹⁶ like transition

points and changing mode of various peaks. PCMW 2D maps also exist in pairs. Moreover, PCMW can also determine the transition temperature regions by peaks in asynchronous map.

Table 2. Change Sequences of Peaks within the $\nu(\text{O}-\text{H})$ Region, $\nu(\text{C}-\text{H})$ Region, and Their Cross Regions Calculated from 2D Maps and Slice Spectra of Figure 4 during the Heating Process of PVME 30 wt % Aqueous Solution^a

cross peak/ cm ⁻¹	symbol in synchronous map	symbol in asynchronous map	change order/cm ⁻¹
(3666, 3392)	—	+	3392 > 3666
(3442, 3278)	+	—	3278 > 3444
(3442, 3392)	+	—	3392 > 3444
(3666, 3442)	—	+	3442 > 3666
		$3392, 3278 > 3442 > 3666 \text{ cm}^{-1}$	
		$\nu_{\text{as}}(\text{OH}), \nu_{\text{s}}(\text{OH})$ in 1:2 adduct $> \nu(\text{bonded O}-\text{H})$ in 1:1 adduct $> \nu(\text{free O}-\text{H})$ in 1:1 adduct (also considered as in free water)	
(2996, 2973)	—	—	2996 > 2973
(2950, 2924)	—	—	2950 > 2924
(2996, 2950)	+	+	2996 > 2950
(2973, 2924)	+	—	2924 > 2973
		$2996 > 2950 > 2924 > 2973 \text{ cm}^{-1}$	
		$\nu_{\text{as}}(\text{hydrated CH}_3) > \nu_{\text{as}}(\text{hydrated CH}_2) > \nu_{\text{as}}(\text{dehydrated CH}_2) > \nu_{\text{as}}(\text{dehydrated CH}_3)$ $> \nu_{\text{as}}(\text{OH}), \nu_{\text{s}}(\text{OH})$ in 1:2 adduct $> \nu(\text{bonded O}-\text{H})$ in 1:1 adduct $> \nu(\text{free O}-\text{H})$ in 1:1 adduct (also considered as in free water)	
(2973, 3392)	—	—	2973 > 3392
		$2996 > 2950 > 2924 > 2973 > 3392 > 3442 > 3666 \text{ cm}^{-1}$	
		$\nu_{\text{as}}(\text{hydrated CH}_3) > \nu_{\text{as}}(\text{hydrated CH}_2) > \nu_{\text{as}}(\text{dehydrated CH}_2) > \nu_{\text{as}}(\text{dehydrated CH}_3)$ $> \nu_{\text{as}}(\text{OH}), \nu_{\text{s}}(\text{OH})$ in 1:2 adduct $> \nu(\text{bonded O}-\text{H})$ in 1:1 adduct $> \nu(\text{free O}-\text{H})$ in 1:1 adduct (also considered as in free water)	

^a According to the assignments, corresponding change sequences of various microstructures are also shown. (“>” means the former peak changes prior to the latter one).

Take PCMW maps in this Article, for example: the *x*-axis is wavenumber and *y*-axis is temperature. The correlation peak ($\nu_1 \text{ cm}^{-1}$, $a \text{ }^\circ\text{C}$) in the synchronous map tells us that $a \text{ }^\circ\text{C}$ is the transition temperature of peak ν_1 , whereas a pair of correlation peaks with the same wavenumber in the asynchronous map, ($\nu_1 \text{ cm}^{-1}$, $b \text{ }^\circ\text{C}$) and ($\nu_1 \text{ cm}^{-1}$, $c \text{ }^\circ\text{C}$) tells us that peak ν_1 starts to change at $b \text{ }^\circ\text{C}$ and ends at $c \text{ }^\circ\text{C}$. Moreover, according to symbols of correlation peaks in both PCMW maps, we can infer the changing style of peak ν_1 . For example, when the correlation peak is: (1) positive in both maps, we can infer peak ν_1 changes in style; (2) positive in synchronous map and negative in asynchronous map, it changes like ; (3) negative in both maps, it changes like ; (4) negative in synchronous map and positive in asynchronous map, it changes like ¹⁶.

A. O–H Stretching Vibration Region. 2DIR Analysis. 2DIR maps obtained during the heating process of PVME 30 wt % aqueous solution are shown in Figure 4, in which information about the $\nu(\text{OH})$ region, the $\nu(\text{CH})$ region, and their cross regions can be found. On the basis of the 2D analysis in the $\nu(\text{OH})$ region, we are able to understand the dynamic variations of different OH vibrations in 1:1 and 1:2 adducts^{3a} during the phase separation process of PVME aqueous solution. There are two autopaks in the synchronous map of $\nu(\text{OH})$ region, 3666 and 3392 cm^{-1} , which are, respectively, assigned to free O–H in the 1:1 adduct and $\nu_{\text{as}}(\text{OH})$ in the 1:2 adduct.³ The appearance of these two autopaks illuminates the fact that both 1:1 and 1:2 adducts perform great changes in the phase separation process. Additionally, the negative cross peak at (3666, 3392) cm^{-1} tells us that these two peaks change toward opposite directions during the heating process.

In the corresponding asynchronous map, there are two major cross peaks (3666, 3392) and (3442, 3278) cm^{-1} ; the former one is positive, whereas the latter one is negative. 3442 cm^{-1} is assigned to bonded O–H in 1:1 adduct, and 3278 cm^{-1} is assigned to $\nu_{\text{s}}(\text{OH})$ in 1:2 adduct.³ The cross peak between these

two peaks also confirms that 1:1 and 1:2 adducts change greatly in the phase separation process.

For further understanding changing sequences of different OH vibrations in PVME–water adducts, we read symbols of cross peaks among the above four peaks in both 2D synchronous and asynchronous maps and sum up the conclusions in Table 2 according to Noda's rule.¹¹ Hence, the thermal-induced changing sequences of four different OH vibrations can be concluded as: $\nu_{\text{as}}(\text{OH}), \nu_{\text{s}}(\text{OH})$ in 1:2 adduct $> \nu(\text{bonded O}-\text{H})$ in 1:1 adduct $> \nu(\text{free O}-\text{H})$ in 1:1 adduct. As we mentioned above, the free OH vibration is similar to the OH vibration in free water molecules, and thus we can consider the changing information of $\nu(\text{free O}-\text{H})$ in 1:1 adduct as that of the free water. From these changing orders, we can understand that during the phase separation process of PVME 30 wt % aqueous solution, the 1:2 adduct formed by PVME and water collapses first, and then it transfers into the 1:1 adduct, whereas with further heating, the 1:1 adduct also dissociates and releases free water molecules. With the help of powerful 2DIR method, we clearly follow this interesting transformation process of hydrogen bonds. Moreover, we also observe from these orders that during heating changes of $\nu(\text{OH})$ start from low wavenumbers and shift to the high wavenumbers; this phenomenon actually reflects the weakening/dissociation of O–H hydrogen bonds, which is exactly the same with blue shifts we observed in Figures 2b and 3a.

PCMW 2DIR Analysis. To obtain the critical changing conditions of O–H hydrogen bonds more accurately, we use PCMW 2DIR method to analyze in the following part. The cross peak in the synchronous map tells the transition point of the peak, whereas cross peaks in the asynchronous map tell when the peak starts and ends its change. Figure 5 shows the PCMW 2DIR maps in $\nu(\text{OH})$ and $\nu(\text{CH})$ regions obtained during the phase separation process of PVME 30 wt % aqueous solution. Two peaks with the wavenumbers of 3666 and 3392 cm^{-1} appear in both synchronous and asynchronous maps of $\nu(\text{OH})$ region,

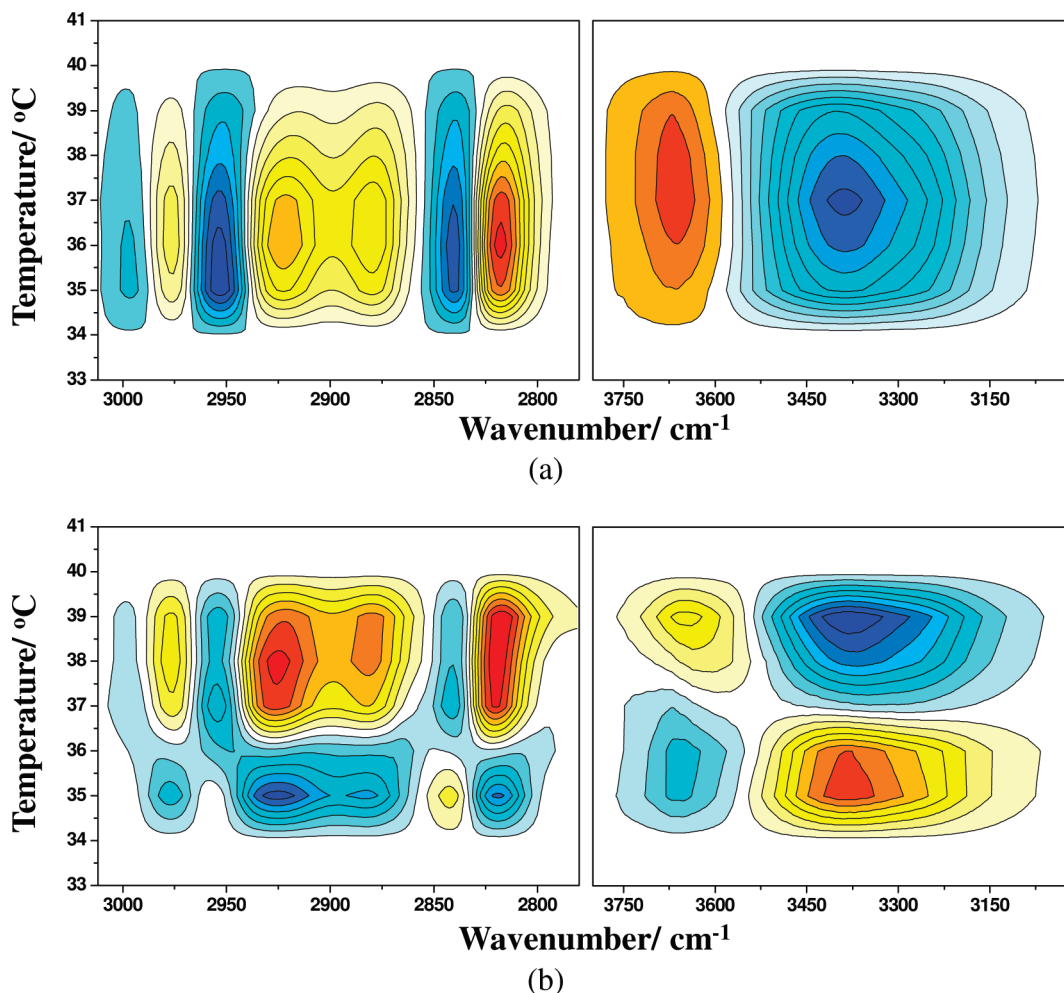


Figure 5. (a) Synchronous and (b) asynchronous PCMW 2DIR maps in the $\nu(\text{OH})$ region and the $\nu(\text{CH})$ region obtained during the phase separation process of PVME 30 wt % aqueous solution.

showing changes of $\nu(\text{free OH})$ in 1:1 adduct (free water) and $\nu_{\text{as}}(\text{OH})$ in 1:2 adduct. For clarity, we list correlation peaks of PCMW maps in Table 3.

We can observe that during phase separation the O–H

hydrogen bond in the 1:2 adduct changes like
35.5 °C → 37 °C → 39 °C,
namely, it dissociates between 35.5 and 39 °C, whereas it changes fastest at 37 °C. Free OH in 1:1 adduct (free water) changes like
37.5 °C → 39 °C. The transition point of the former one 37 °C is

lower than that of the latter one 37.5 °C, which also testifies that during the phase separation process the 1:2 adduct transfers to 1:1 adduct and gradually releases free water molecule. Therefore, from the consistency of conclusions in 2DIR and PCMW analysis, we can clearly observe the thermal-induced dissociation behaviors of O–H hydrogen bonds structures in the PVME 30 wt % aqueous solution.

B. C–H Stretching Vibration Region. 2DIR Analysis. 2DIR maps in $3012\text{--}2780\text{ cm}^{-1}$ of Figure 4 also help us investigate changing orders of the C–H groups. There are seven autopeaks in the synchronous map centered at 2996, 2973, 2950, 2924, 2879, 2839, and 2817 cm^{-1} . According to their assignments in Table 1, we can observe that 2996 and 2973 cm^{-1} are assigned to

the hydrated and dehydrated $\nu_{\text{as}}(\text{CH}_3)$; 2839 and 2817 cm^{-1} are assigned to the hydrated and dehydrated $\nu_s(\text{CH}_3)$; 2950 and 2924 cm^{-1} are assigned to the hydrated and dehydrated $\nu_{\text{as}}(\text{CH}_2)$; whereas 2879 cm^{-1} is assigned to the hydrated $\nu_s(\text{CH}_2)$. The appearance of these autopeaks manifests hydration states of CH_3 and CH_2 undergo great changes during phase separation of PVME 30 wt % aqueous solution. There are many cross peaks among these peaks in 2DIR maps; to be more clear, because both pairs of 2996/2973 and 2839/2817 cm^{-1} are related to the hydration/dehydration states of CH_3 , we take the pair of 2996/2973 cm^{-1} as an example to study the change of CH_3 . Similarly, we choose 2950/2924 cm^{-1} to study the change of CH_2 . Symbols of cross peaks in 2D maps and the concluded changing orders of various microstructures are summed up in Table 2. Therefore, the thermal-induced changing sequences of CH_3 and CH_2 groups can be inferred as: $\nu_{\text{as}}(\text{hydrated CH}_3) > \nu_{\text{as}}(\text{hydrated CH}_2) > \nu_{\text{as}}(\text{dehydrated CH}_2) > \nu_{\text{as}}(\text{dehydrated CH}_3)$; namely, during the phase separation process of PVME 30 wt % aqueous solution, the initially hydrated CH_3 starts its dehydration first, and then the initially hydrated CH_2 also starts to dehydrate. Whereas the whole dehydration process of CH_2 completes very fast, it starts later but ends even earlier than that of the CH_3 , which is coherent with Maeda's publication.^{9a}

Table 3. Correlation Peaks and Their Symbols in PCMW 2DIR Maps of Figure 5 in the $\nu(\text{OH})$ and $\nu(\text{CH})$ Regions during the Phase Separation Process of PVME 30 wt % Aqueous Solution^a

Correlation peaks and their symbols in synchronous map/ (cm ⁻¹ , °C)	Correlation peaks and their symbols in asynchronous map/ (cm ⁻¹ , °C)	Changing styles of peaks
(3666, 37.5) +	(3666, 35.5) -	
	(3666, 39) +	
(3392, 37) -	(3392, 35.5) +	
	(3392, 39) -	
(2973, 36.5) +	(2973, 35) -	
	(2973, 38) +	
(2919, 36.5) +	(2919, 35) -	
	(2919, 38) +	

^a Accordingly concluded changing styles of peaks are also shown.

PCMW 2DIR Analysis. We also use the PCMW method to study the changing conditions of CH_3 and CH_2 in Figure 5. We can see that in the synchronous map within $3012\text{--}2780\text{ cm}^{-1}$, there are seven correlation peaks. Negative peaks at (2996 cm^{-1} , $35.5\text{ }^\circ\text{C}$), (2950 cm^{-1} , $35.5\text{ }^\circ\text{C}$), and (2839 cm^{-1} , $35.5\text{ }^\circ\text{C}$) indicate that the hydrated CH_3 and CH_2 undergo dehydration processes fastest at $35.5\text{ }^\circ\text{C}$, whereas positive correlation peaks at (2973 cm^{-1} , $36.5\text{ }^\circ\text{C}$), (2924 cm^{-1} , $36.5\text{ }^\circ\text{C}$), (2879 cm^{-1} , $36.5\text{ }^\circ\text{C}$), and (2817 cm^{-1} , $36.5\text{ }^\circ\text{C}$) indicate that formations of dehydrated CH_3 and CH_2 happen fastest at $36.5\text{ }^\circ\text{C}$, which is $1\text{ }^\circ\text{C}$ higher than the transition point of dehydration processes. Therefore, we can infer that the transition from hydrated C-H groups to the dehydrated ones is a time-consuming process. There might be many intermediates; the higher the temperature, fewer water molecules could hydrate with the CH_3 and CH_2 groups.

For clarity, we take 2973 and 2924 cm^{-1} as examples and also list all of their correlation peaks in Table 3 to study changes of CH_3 and CH_2 groups during the phase separation process. From Table 3, we can conclude that both dehydrated state CH_3 and CH_2 appear from $35\text{ }^\circ\text{C}$, then achieve their fastest rate of rise at $36.5\text{ }^\circ\text{C}$, and eventually end their rise at $38\text{ }^\circ\text{C}$.

The entire increase process goes like

comparison of PCMW 2D analysis in $\nu(\text{OH})$ and $\nu(\text{CH})$ regions, we can note that the transition temperature of hydrophobic groups is $\sim 36.5\text{ }^\circ\text{C}$, whereas that of the hydrophilic group is $\sim 37.5\text{ }^\circ\text{C}$, which roughly points out that the hydrophobic groups change prior to hydrophilic group within the phase separation process. To confirm this further, we will make 2D cross regions analysis between $\nu(\text{OH})$ and C-H regions in Section D.

C. $\text{CH}_3\text{--O}$ Stretching Vibration Region. 2DIR Analysis. As a supplement for the $\nu(\text{O-H})$ region, we investigate the $\nu(\text{CH}_3\text{--O})$ region by 2DIR analysis in Figure 6. There are

two autopeaks in the synchronous map, centered at 1066 and 1095 cm^{-1} , which are assigned to $\nu(\text{CH}_3\cdots\text{water})$ and $\nu(\text{free CH}_3\text{--O})$, respectively. Cross peak ($1095, 1066\text{ cm}^{-1}$) is negative in the synchronous map but positive in the asynchronous map; according to Noda's rule,¹¹ we can infer $1066 > 1095\text{ cm}^{-1}$. Namely, during the phase separation, hydrogen bonds between $\text{CH}_3\text{--O}$ and water will dissociate and release free $\text{CH}_3\text{--O}$ group. This is consistent with our conclusion in the 2DIR analysis of the $\nu(\text{OH})$ region; both parts confirm the breakage of hydrogen bonds formed between water and the hydrophilic group of PVME and therefore release free water molecules and free $\text{CH}_3\text{--O}$ groups after the heating-induced phase separation process of PVME 30 wt % aqueous solution. As we mentioned above, CaF_2 is used as the window material in FTIR experiments; only spectra information above 1100 cm^{-1} is accurate. Therefore, the result of the $\nu(\text{CH}_3\text{--O})$ region is just considered to be a supplement, and PCMW analysis has not been done in this work.

D. C-H versus O-H Stretching Vibration Region. 2DIR Analysis. On the basis of 2DIR analysis of $\nu(\text{OH})$ region in Section A, we have concluded transformation orders of various O-H hydrogen bonds as $3392, 3278 > 3442 > 3666\text{ cm}^{-1}$; whereas in 2DIR analysis of the $\nu(\text{CH})$ region in part B, we have obtained dehydration orders among hydrophobic C-H groups to be $2996 > 2950 > 2924 > 2973\text{ cm}^{-1}$. For further comparison of changing sequences between the dissociation of hydrophilic-group-involved hydrogen bonds and dehydration of hydrophobic groups, we cross-correlate these two regions also in Figure 4. Because of the negative cross peak at ($2973, 3392\text{ cm}^{-1}$) in both maps, we can link changing orders obtained in Sections A and B as follows: $2996 > 2950 > 2924 > 2973 > 3392 > 3442 > 3666\text{ cm}^{-1}$, indicating that during heating the initially hydrated state hydrophobic groups undergo dehydration first, and then the hydrophilic group gets rid of its hydrogen bonds between water

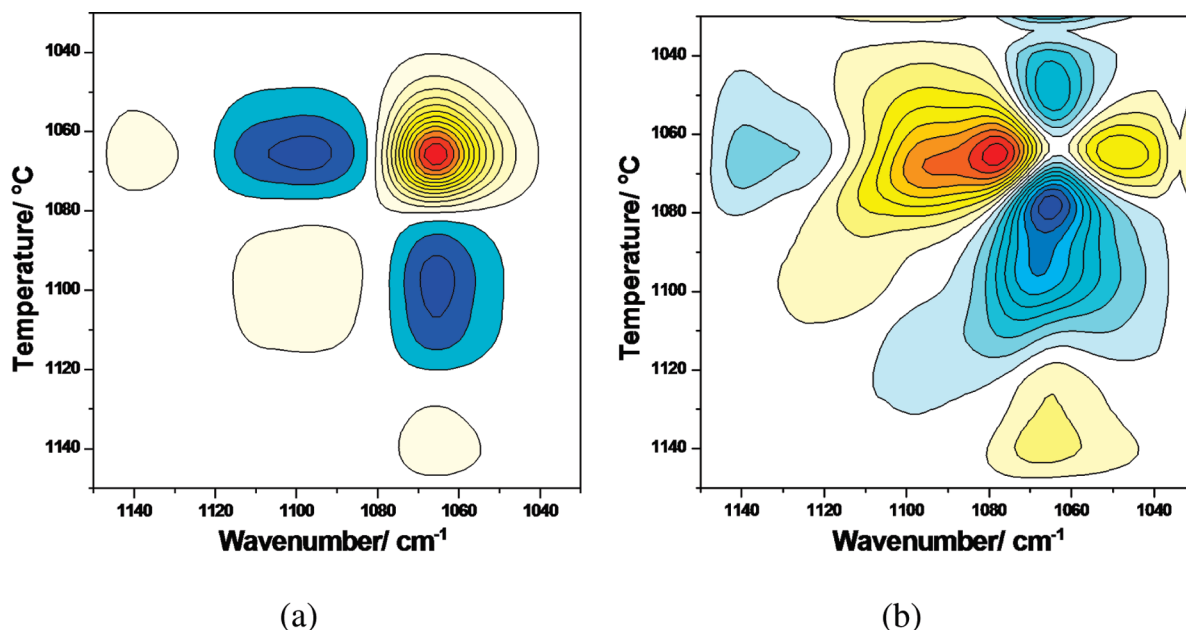
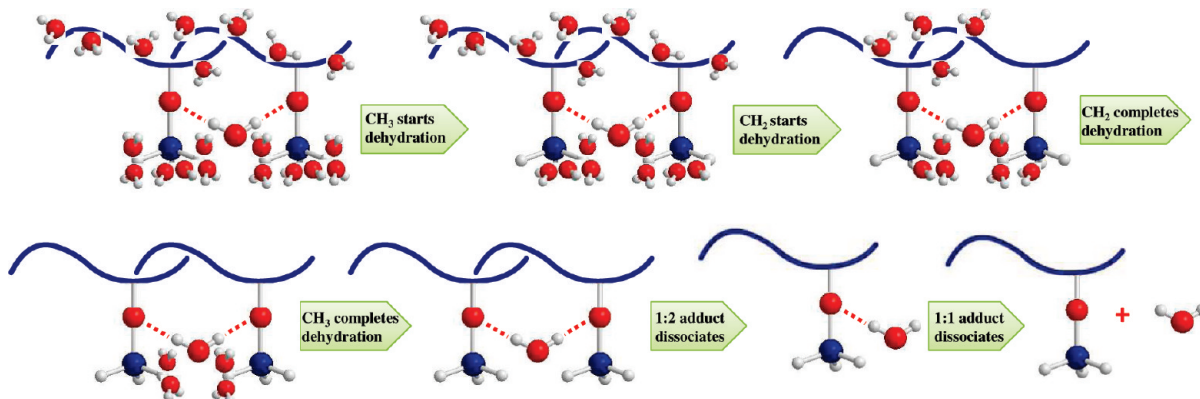


Figure 6. (a) Synchronous and (b) asynchronous maps of the $\nu(\text{CH}_3-\text{O})$ region obtained during the phase separation process of PVME 30 wt % aqueous solution.

Scheme 1. Entire Microdynamic Mechanism of PVME 30 wt % Aqueous Solution Phase Separation Process^a



^a During heating, the initially hydrated state CH_3 starts to dehydrate as the first action, and initially hydrated CH_2 follows; to start their dehydration, interestingly, water molecules leave CH_2 very fast, and the whole dehydration process of CH_2 ends even earlier than that of CH_3 . After hydrophobic groups finish dehydrations, hydrogen bonds between hydrophilic group and water start to dissociate. 1:2 adducts formed between PVME and water dissociate first and transfer into 1:1 adducts, whereas with further heating 1:1 adducts eventually dissociate and release free water molecules and free CH_3-O group. (The number of water molecules surrounding C-H groups is not exact, it is only approximately drawn to describe the dehydration process of CH_3 and CH_2 groups, and sizes of all structures are adjusted for better appearance.).

molecules. This is exactly the same with what we have concluded in PCMW 2D analysis above.

In summary, we are able to conclude clearly the entire microdynamic mechanism of PVME 30 wt % aqueous solution phase separation process. The temperature rise induces the initially hydrated state CH_3 groups to start to dehydrate as the first action of phase separation, and the initially hydrated state CH_2 follows that to start its dehydration. Interestingly, water molecules leave CH_2 very fast, and the whole dehydration process of CH_2 ends even earlier than that of CH_3 . After hydrophobic groups finish their dehydration processes, hydrogen bonds between hydrophilic group and water start to dissociate. 1:2 adducts formed between PVME and water dissociate first and transfer to the 1:1 adducts, whereas with further

heating, 1:1 adducts eventually dissociate and release free water molecules and free CH_3-O group. This sequence is illustrated clearly in Scheme 1.

The hydrophobic groups change prior to the hydrophilic group of PVME during the phase separation process of PVME 30 wt % aqueous solution; this changing order is the same as the phase separation mechanism of PNIPAM 20 wt % D_2O solution in our previous study.^{12d} However, in PVME aqueous solution of various concentrations, whether the changing orders between various structures might be different still needs further study. Therefore, we can conclude that concentrations have great influence on the phase separation mechanism of PNIPAM aqueous solution. In future work, we will continue to study

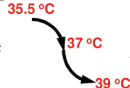
whether there is similar concentration dependence in the phase separation processes of PVME aqueous solutions.

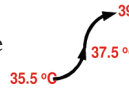
CONCLUSIONS

We have used FTIR spectra to study the phase separation and the reverse process of PVME 30 wt % aqueous solution during the heating-and-cooling cycle. The O—H, C—H, and CH₃—O stretching vibration regions are investigated in detail. For the hydrophilic group, we quantitatively analyze the temperature dependence of ν(OH) positions, finding that the dissociation and formation of hydrogen bonds between hydrophilic group and water (CH₃—O···water) during heating and cooling processes are reversible without any hysteresis. For hydrophobic groups, we quantitatively analyze the temperature dependence of positions of ν_{as}(CH₂) and also prove the complete reversibility of dehydration during heating and hydration during cooling of hydrophobic groups.

For clearly understanding the microdynamics mechanism of phase separation behavior of PVME 30 wt % aqueous solution, we have used the 2DIR technique, concluding that during heating the initially hydrated CH₃ groups start to dehydrate as the first action of phase separation, and the initially hydrated CH₂ follows to start its dehydration. Interestingly, water molecules leave CH₂ very fast, and the whole dehydration process of CH₂ ends even earlier than that of CH₃. After hydrophobic groups finish their dehydrations, hydrogen bonds between hydrophilic group and water start to dissociate. 1:2 adducts formed between PVME and water dissociate first and transfer to the 1:1 adducts, whereas with further heating, 1:1 adducts eventually dissociate and release free water and free CH₃—O.

As supplements, we use PCMW 2DIR analysis to understand further changing conditions of various microstructures. We observe that during the phase separation, the O—H hydrogen

bond in 1:2 adduct changes like , which means it dissociates between 35.5 and 39 °C and changes fastest at 37 °C, whereas free OH in 1:1 adduct (also considered as free water)

changes like , which changes later than the 1:2 adduct. Meanwhile, we also investigate dehydration conditions of hydrophobic groups, finding that both dehydrated CH₃ and CH₂ appear from 35 °C, then achieve their fastest rate of rise at 36.5 °C, and eventually end increasing at 38 °C. The entire

increase process goes like . From the results of

PCMW and 2DIR analysis, microdynamic change orders of hydrophobic and hydrophilic groups are further confirmed.

AUTHOR INFORMATION

Corresponding Author

*E-mail: Peiyiwu@fudan.edu.cn.

ACKNOWLEDGMENT

We gratefully acknowledge the financial support of the National Science Foundation of China (NSFC) (20934002, 20774022) and the National Basic Research Program of China (No. 2009CB930000).

REFERENCES

- (a) Berge, B.; Koningsveld, R.; Berghmans, H. Influence of added components on the miscibility behavior of the (quasi-)binary system water poly(vinyl methyl ether) and on the swelling behavior of the corresponding hydrogels. I. Tetrahydrofuran. *Macromolecules* **2004**, *37*, 8082–8090. (b) Kharlampieva, E.; Kozlovskaya, V.; Tyutina, J.; Sukhishvili, S. A. Hydrogen-bonded multilayers of thermoresponsive polymers. *Macromolecules* **2005**, *38*, 10523–10531. (c) Loozen, E.; Nies, E.; Heremans, K.; Berghmans, H. The influence of pressure on the lower critical solution temperature miscibility behavior of aqueous solutions of poly(vinyl methyl ether) and the relation to the compositional curvature of the volume of mixing. *J. Phys. Chem. B* **2006**, *110*, 7793–7802. (d) Van Durme, K.; Loozen, E.; Nies, E.; Van Mele, B. Phase behavior of poly(vinyl methyl ether) in deuterium oxide. *Macromolecules* **2005**, *38*, 10234–10243. (e) Van Durme, K.; Rahier, H.; Van Mele, B. Influence of additives on the thermoresponsive behavior of polymers in aqueous solution. *Macromolecules* **2005**, *38*, 10155–10163. (f) Van Durme, K.; Van Assche, G.; Nies, E.; Van Mele, B. Phase transformations in aqueous low molar mass poly(vinyl methyl ether) solutions: theoretical prediction and experimental validation of the peculiar solvent melting line, bimodal LCST, and (adjacent) UCST miscibility gaps. *J. Phys. Chem. B* **2007**, *111*, 1288–1295.

- (a) Frank, H. S.; Evans, M. W. Free volume and entropy in condensed systems 0.3. Entropy in binary liquid mixtures - partial molal entropy in dilute solutions - structure and thermodynamics in aqueous electrolytes. *J. Chem. Phys.* **1945**, *13*, 507–532. (b) Israelachvili, J.; Pashley, R. The hydrophobic interaction is long-range, decaying exponentially with distance. *Nature* **1982**, *300*, 341–342. (c) Nemethy, G.; Scheraga, H. A. Structure of water and hydrophobic bonding in proteins 0.2. model for thermodynamic properties of aqueous solutions of hydrocarbons. *J. Chem. Phys.* **1962**, *36*, 3401–&. (d) Stillinger, F. H. Water revisited. *Science* **1980**, *209*, 451–457. (e) Cho, E. C.; Lee, J.; Cho, K. Role of bound water and hydrophobic interaction in phase transition of poly(N-isopropylacrylamide) aqueous solution. *Macromolecules* **2003**, *36*, 9929–9934. (f) Inomata, H.; Goto, S.; Saito, S. Phase-transition of N-substituted acrylamide gels. *Macromolecules* **1990**, *23*, 4887–4888. (g) Otake, K.; Inomata, H.; Konno, M.; Saito, S. Thermal-analysis of the volume phase-transition with N-isopropylacrylamide gels. *Macromolecules* **1990**, *23*, 283–289.

- (a) Guo, Y. L.; Sun, B. J.; Wu, P. Y. Phase separation of poly(vinyl methyl ether) aqueous solution: a near-infrared spectroscopic study. *Langmuir* **2008**, *24*, 5521–5526. (b) Bryan, S. A.; Willis, R. R.; Moyer, B. A. Hydration of 18-crown-6 in carbon-tetrachloride - infrared spectral evidence for an equilibrium between monodentate and bidentate forms of bound water in the 1–1 crown water adduct. *J. Phys. Chem.* **1990**, *94*, 5230–5233. (c) Sammon, C.; Mura, C.; Yarwood, J.; Everall, N.; Swart, R.; Hodge, D. FTIR-ATR studies of the structure and dynamics of water molecules in polymeric matrixes. A comparison of PET and PVC. *J. Phys. Chem. B* **1998**, *102*, 3402–3411.

- (a) Hanykova, L.; Spevacek, J.; Ilavsky, M. ¹H NMR study of thermotropic phase transition of linear and crosslinked poly(vinyl methyl ether) in D₂O. *Polymer* **2001**, *42*, 8607–8612. (b) Spevacek, J.; Hanykova, L.; Ilavsky, M. Polymer-solvent interactions during phase transition in poly(vinyl methyl ether)/D₂O solutions as studied by NMR methods. *Macromol. Symp.* **2001**, *166*, 231–236. (c) Spevacek, J.; Hanykova, L. ¹H NMR relaxation study of polymer-solvent interactions during thermotropic phase transition in aqueous solutions. *Macromol. Symp.* **2003**, *203*, 229–237. (d) Spevacek, J.; Hanykova, L.; Starovoytova, L. ¹H NMR relaxation study of thermotropic phase transition in poly(vinyl methyl ether)/D₂O solutions. *Macromolecules* **2004**, *37*, 7710–7718. (e) Spevacek, J.; Hanykova, L. ¹H NMR study on the hydration during temperature-induced phase separation in concentrated poly(vinyl methyl ether)/D₂O solutions. *Macromolecules* **2005**, *38*, 9187–9191.

- (f) Okano, K.; Takada, M.; Kurita, K.; Furusaka, M. Interaction parameters of poly(vinyl methyl-ether) in aqueous-solution as determined by small-angle neutron-scattering. *Polymer* **1994**, *35*, 2284–2289.

- (6) (a) Cerveny, S.; Colmenero, J.; Alegria, A. Dielectric investigation of the low-temperature water dynamics in the poly(vinyl methyl ether)/H₂O system. *Macromolecules* **2005**, *38*, 7056–7063. (b) Shinyashiki, N.; Matsumura, Y.; Mashimo, S.; Yagihara, S. Dielectric study on coupling constant of lower critical solution of poly(vinylmethylether) in water. *J. Chem. Phys.* **1996**, *104*, 6877–6880.
- (7) (a) Zhang, J. M.; Berge, B.; Meeussen, F.; Nies, E.; Berghmans, H.; Shen, D. Y. Influence of the interactions in aqueous mixtures of poly(vinyl methyl ether) on the crystallization behavior of water. *Macromolecules* **2003**, *36*, 9145–9153. (b) Loozen, E.; Van Durme, K.; Nies, E.; Van Mele, B.; Berghmans, H. The anomalous melting behavior of water in aqueous PVME solutions. *Polymer* **2006**, *47*, 7034–7042.
- (8) (a) Tamai, Y.; Tanaka, H.; Nakanishi, K. Molecular dynamics study of polymer-water interaction in hydrogels 0.1. hydrogen-bond structure. *Macromolecules* **1996**, *29*, 6750–6760. (b) Tamai, Y.; Tanaka, H.; Nakanishi, K. Molecular dynamics study of polymer-water interaction in hydrogels 0.2. Hydrogen-bond dynamics. *Macromolecules* **1996**, *29*, 6761–6769. (c) Zeng, X. G.; Yang, X. Z. A study of interaction of water and model compound of poly(vinyl methyl ether). *J. Phys. Chem. B* **2004**, *108*, 17384–17392.
- (9) (a) Maeda, Y.; Mochiduki, H.; Yamamoto, H.; Nishimura, Y.; Ikeda, I. Effects of ions on two-step phase separation of poly(vinyl methyl ether) in water as studied by IR and Raman spectroscopy. *Langmuir* **2003**, *19*, 10357–10360. (b) Pastorcak, M.; Kozanecki, M.; Ulanski, J. Water-polymer interactions in PVME hydrogels - Raman spectroscopy studies. *Polymer* **2009**, *50*, 4535–4542.
- (10) (a) Gu, W. X.; Wu, P. Y. FT-IR and 2D-IR spectroscopic studies on the effect of ions on the phase separation behavior of PVME aqueous solution. *Anal. Sci.* **2007**, *23*, 823–827. (b) Maeda, H. Interaction of water with poly(vinyl methyl-ether) in aqueous-solution. *J. Polym. Sci., Part B: Polym. Phys.* **1994**, *32*, 91–97. (c) Maeda, Y. IR spectroscopic study on the hydration and the phase transition of poly(vinyl methyl ether) in water. *Langmuir* **2001**, *17*, 1737–1742. (d) Zhang, T. Z.; Nies, E.; Todorova, G.; Li, T.; Berghmans, H.; Ge, L. Q. Isothermal crystallization kinetics study on aqueous solution of poly(vinyl methyl ether) by FTIR and optical microscopy method. *J. Phys. Chem. B* **2008**, *112*, 5611–5615. (e) Zhang, J. M.; Zhang, G. B.; Wang, J. J.; Lu, Y. L.; Shen, D. Y. Infrared spectroscopic study on the crystallization of water in poly(vinyl methyl ether) aqueous solution during heating. *J. Polym. Sci., Part B: Polym. Phys.* **2002**, *40*, 2772–2779.
- (11) (a) Noda, I. Generalized 2-dimensional correlation method applicable to infrared, Raman, and other types of spectroscopy. *Appl. Spectrosc.* **1993**, *47*, 1329–1336. (b) Noda, I.; Story, G. M.; Marcott, C. Pressure-induced transitions of polyethylene studied by two-dimensional infrared correlation spectroscopy. *Vib. Spectrosc.* **1999**, *19*, 461–465. (c) Noda, I. Determination of two-dimensional correlation spectra using the Hilbert transform. *Appl. Spectrosc.* **2000**, *54*, 994–999.
- (12) (a) Segtnan, V. H.; Sasic, S.; Isaksson, T.; Ozaki, Y. Studies on the structure of water using two-dimensional near-infrared correlation spectroscopy and principal component analysis. *Anal. Chem.* **2001**, *73*, 3153–3161. (b) Wu, P.; Siesler, H. W. Two-dimensional correlation analysis of variable-temperature Fourier-transform mid- and near-infrared spectra of polyamide 11. *J. Mol. Struct.* **2000**, *521*, 37–47. (c) Sun, B. J.; Lin, Y. A.; Wu, P. Y. Structure analysis of poly(N-isopropylacrylamide) using near-infrared spectroscopy and generalized two-dimensional correlation infrared spectroscopy. *Appl. Spectrosc.* **2007**, *61*, 765–771. (d) Sun, B. J.; Lin, Y. N.; Wu, P. Y.; Siesler, H. W. A FTIR and 2D-IR spectroscopic study on the microdynamics phase separation mechanism of the poly(N-isopropylacrylamide) aqueous solution. *Macromolecules* **2008**, *41*, 1512–1520.
- (13) (a) Sasic, S.; Amari, T.; Ozaki, Y. Sample-sample and wave-number-wavenumber two-dimensional correlation analyses of attenuated total reflection infrared spectra of polycondensation reaction of bis(hydroxyethylterephthalate). *Anal. Chem.* **2001**, *73*, 5184–5190. (b) Shen, Y.; Wu, P. Y. Two-dimensional ATR-FTIR spectroscopic investigation on water diffusion in polypropylene film: water bending vibration. *J. Phys. Chem. B* **2003**, *107*, 4224–4226.
- (14) Jonsson, J.; Persson, P.; Sjoberg, S.; Lovgren, L. Schwertmannite precipitated from acid mine drainage: phase transformation, sulphate release and surface properties. *Appl. Geochem.* **2005**, *20*, 179–191.
- (15) Lopez-Diez, E. C.; Winder, C. L.; Ashton, L.; Currie, F.; Goodacre, R. Monitoring the mode of action of antibiotics using Raman spectroscopy: Investigating subinhibitory effects of amikacin on *Pseudomonas aeruginosa*. *Anal. Chem.* **2005**, *77*, 2901–2906.
- (16) Morita, S.; Shinzawa, H.; Noda, I.; Ozaki, Y. Perturbation-correlation moving-window two-dimensional correlation spectroscopy. *Appl. Spectrosc.* **2006**, *60*, 398–406.
- (17) SchaferSoenen, H.; Moerkerke, R.; Berghmans, H.; Koningsveld, R.; Dusek, K.; Solc, K. Zero and off-zero critical concentrations in systems containing polydisperse polymers with very high molar masses 0.2. The system water-poly(vinyl methyl ether). *Macromolecules* **1997**, *30* (3), 410–416.